IMPACT OF POLY (SODIUM-4-STYRENE SULFONATE) CONCENTRATION ON CELLULOSE TRIACETATE BASED MEMBRANE STRUCTURE AND PERFORMANCE

SOFIANE BENSADI,[*] YASSINE BERBAR,[*] MOURAD AMARA,[*,**] OMAR AROUS,[*] HIBA FERHAT[***] and FAIROUZ SAAD SAOUD[*]

[*]*Laboratory of Hydrometallurgy and Molecular Inorganic Chemistry, Faculty of Chemistry, USTHB, PO Box 32 El Alia Algiers 16111 Algeria*
[**]*National School of Nanosciences and Nanotechnology, Algiers, Algeria*
[***]*Laboratory of Electrochemistry, Corrosion, Metallurgy, and Mineral Chemistry, Faculty of Chemistry, USTHB, PO Box 32 El Alia Algiers 16111 Algeria*
✉ *Corresponding author: O. Arous, omararous@yahoo.fr*

Received June 25, 2025

This work investigated the effects of using poly(sodium-4-styrene sulfonate) (PSS) as a novel polymer additive on cellulose triacetate-based membranes (CTA), applied for the treatment of saline solutions containing Na^+, K^+, and Ca^{2+} ions. New membranes composed of a mixture of CTA, PSS with different concentrations and di-(2-ethyl hexyl) phosphoric acid (D2EHPA) as a plasticizer, were elaborated. The dialysis process was used for evaluating the impact of PSS concentration on the membranes' performance, using both synthetic saline and seawater solutions. Various physical properties of the membranes were highlighted by different characterization techniques, such as Fourier-transform infrared spectroscopy (FTIR) and scanning electron microscopy (SEM). Characterization results showed that PSS integrated into the membrane matrix can act as a morphology modifier by pushing D2EHPA from the inside to the surface of the membrane. Application results indicated that the transfer efficiencies increased with higher amounts of PSS in the membrane. The highest removal efficiencies observed were 49.74%, 44.39%, and 3.74% for K^+, $Ca^{2+}$and Na^+ ions, respectively, using synthetic solutions. For seawater solutions, the removal efficiencies were slightly lower: at 33.58%, 29.95%, and 2.20% for K^+, Ca^{2+} and Na^+ ions, respectively. The membrane with PSS effectively promotes the removal of ions, leading to a reduction in conductivity, salinity, and TDS.

Keywords: membrane, PSS, CTA, polymer dispersion, D2EHPA

INTRODUCTION

Water scarcity is a critical global crisis driven by climate change, population growth and resource mismanagement, affecting agricultural and environmental sustainability. It was expected that, by 2025, almost 2 billion people would face absolute water scarcity, while two-thirds of the world could experience water stress. Key solutions include advanced irrigation, wastewater recycling, and desalination technologies.[1-3] Over the past few decades, seawater desalination appears as one of the most efficient and effective processes for producing high-quality drinking water.[4,5] This process is particularly vital in arid regions, where water insufficiency affects more households, industries, and agriculture.[6-8] Seawater treatment using advanced techniques, such as multi-effect distillation (MED),[9,10] multi-stage flash (MSF) distillation,[11,12] and reverse osmosis (RO) using membranes[13-15] reveals itself as the most developed solution in this field. Among these, seawater treatment employing membrane processes is considered as the most cost-effective compared to other methods.[16,17]

While it has several advantages, the seawater desalination process using membranes encounters several challenges, including membrane fouling[18,19] caused mainly by the presence of calcium and other organic compounds. Membrane fouling is known to be the major culprit to the elevated operating costs due to the deterioration of

permeate flux, increasing transmembrane pressure, and requiring frequent chemical cleaning, which shorten the membrane's lifecycle.[20]

To improve the efficiency and longevity of reverse osmosis systems, effective pretreatment of seawater is therefore essential.[21] The pretreatment phase can be carried out by conventional methods, such as coagulation, flocculation,[22] and granular filtration,[23] but also filtration on sand and activated carbon;[24,25] however, these methods are insufficient. For this reason, more advanced techniques using membranes are emerging as an important contribution to improving the quality of pretreated seawater.[26,27] Ultrafiltration (UF), nanofiltration (NF) and dialysis processes using polymeric membranes can effectively reduce total dissolved solids (TDS), calcium, magnesium, and organic matter,[28] which are critical contributors to fouling in RO processes.[29,30]

Polymer inclusion membranes (PIMs) have recently been used as an alternative to supported liquid membranes (SLM).[31-37] As the carrier is mixed with the polymer in PIMs, the release of the carrier from the membrane phase to the aqueous phases, which occurs when SLM membrane are used, is avoided. In PIMs, the carrier remains fixed within the membrane matrix, due to the absence of an actual liquid solvent. PIMs are usually composed of a polymer, such as cellulose triacetate (CTA) or polymethyl methacrylate (PMMA), a carrier acting as an extractant that is responsible for providing the specific selectivity for the target analyte; commonly with the addition of a plasticizer to improve maliability and mechanic resistence.

Renowned for its diverse applications and distinctive properties, sodium poly(4-styrene sulfonate) (PSS) is a polymer that has attracted considerable attention in membrane synthesis.[38,39] PSS containing the sulfonate group is known for its ability to introduce negative charges, which can significantly improve membranes antifouling properties and ion selectivity.[40,41] The addition of PSS into membranes improves the overall performance and longevity of membranes, particularly by reducing the biofouling and scaling phenomena encountered in desalination processes.[42,43] The investigation of the impact of specific additives on membrane structure is essential for a comprehensive understanding of membrane performance.[44,45]

In this context, this study was conducted to evaluate the effectiveness of newly synthesized polymeric membranes, incorporating PSS, for saline solution treatment through the dialysis process. The study focuses on the characterization of these membranes in terms of physicochemical properties, surface morphology, and ion transfer efficiency. By optimizing the amount of PSS and other synthesis parameters, we aim to develop membranes with higher performance in terms of salinity and organic impurities reduction, as well as operational stability.

EXPERIMENTAL

Materials

Cellulose triacetate (CTA 72000-74000 g/mol), chloroform (99.8%), poly(sodium-4-styrene sulfonate) (PSS: Mw 70,000 g/mol) were purchased from Sigma Aldrich. The aqueous phases were prepared by dissolving the different reagents in demineralized water. Na^+, K^+, and Ca^{2+} ions concentrations in the synthetic solution were close to the concentration of these ions in seawater (Table 1).

Table 1
Na^+, K^+, and Ca^{2+} ions concentrations in synthetic and seawater solutions

	Na^+	K^+	Ca^{2+}
Synthetic solution (mg/L)	10000	390	410
Seawater solution (mg/L)	10783	393	412

Synthesis and characterization of polymeric membranes

The membrane fabrication employed the solvent evaporation method.[46] Initially, 0.2 g of cellulose triacetate (CTA) was dissolved in 20 mL of chloroform and stirred for 3 hours. Subsequently, 0.1 mL of the plasticizer di-(2-ethylhexyl) phosphoric acid (D2EHPA) was added, and the mixture was stirred for an additional hour. In parallel, 0–0.03 g of poly(sodium-4-styrene sulfonate) (PSS) was dispersed in 20 mL of tetrahydrofuran (THF) and stirred for 1 hour. The resulting CTA solution was then combined with the PSS solution in a 10 cm diameter Petri dish and allowed to undergo slow solvent evaporation for at least 24 hours. The formed membrane was subsequently detached by the addition of distilled water and dried using absorbent paper. The formulations of the membranes, with the amounts of CTA, PSS and D2EHPA, are presented in Table 2.

To elucidate various physical characteristics of the membranes, multiple characterization techniques were employed. FTIR spectra of the prepared membranes were recorded using a Perkin Elmer spectrophotometer (Spectrum One model), in the range of 400-4000 cm^{-1}, with a resolution of 2 cm^{-1}, and a total of 64 scans were accumulated for each spectrum. The surface morphologies of the synthesized membranes were observed via SEM imaging using a Philips Scanning Electron Microscope XL30 FEG (the Netherlands), with a voltage of 20 keV. The contact angle measurements were carried out as the tangent angle of the drop with the membrane surface. Water contact angles were recorded with an OCA20 Data-Physics Instruments, using a syringe to control the droplet size. The average of three arbitrarily selected locations for each sample represents the reported contact angle measurements. Additionally, the different solutions were analyzed using flame spectrophotometry analysis.

Table 2
Formulations of the membranes

Membrane	CTA (g)	PSS (g)	D2EHPA (mL)
M1	0.2	00	0.1
M2	0.2	0.01	0.1
M3	0.2	0.02	0.1
M4	0.2	0.03	0.1

The seawater solution underwent pretreatment via sand filtration to remove any suspended particles that could affect the efficiency of the membranes.

The synthesized membranes were applied to treat aqueous solutions containing ions (Na^+, Ca^{2+}, and K^+) and a seawater sample, using dialysis as the membrane separation process. The dialysis cell consists of two compartments separated by a membrane with an effective surface area of 49 cm^2. The feed compartment contains the solution to be treated. Samples were collected from each compartment using a graduated pipette. The receiving solution can be regenerated by precipitating the ions transferred through the membrane from the treated solution.

RESULTS AND DISCUSSION

Physicochemical properties

Table 3 presents the appearance, the density values and contact angles for the various synthesized membranes. Firstly, the membranes exhibited a homogeneous dispersion of PSS, facilitated by the dual-solvent strategy: chloroform was used to solubilize cellulose triacetate (CTA), while tetrahydrofuran (THF) promoted the dispersion of PSS. The dispersion behavior of polystyrene sulfonate (PSS) in organic solvents is primarily governed by its polyelectrolytic nature and the polarity of the surrounding medium. In its salt form, PSS carries highly hydrophilic sulfonate groups ($–SO_3^–$), which exhibit poor compatibility with low-polarity solvents. Chloroform, with its low dielectric constant ($\varepsilon \approx 4.8$) and limited dipolar character, cannot effectively solvate ionic species. This leads to interchain aggregation through ionic bridging between sulfonate groups and counterions (*e.g.*, Na^+), resulting in phase separation or precipitation. In contrast, THF offers moderate polarity ($\varepsilon \approx 7.6$) and aprotic character, enabling partial stabilization of the charged sulfonate groups via coordination with its electron-rich oxygen atoms. This reduces ionic aggregation and supports better polymer dispersion.

Combining THF and chloroform in mixed-solvent systems can synergize the solubility requirements of both hydrophilic (PSS) and hydrophobic (CTA) components. Such solvent mixtures are especially useful for preparing homogeneous polymer blends and membranes where interfacial compatibility is crucial.

The density was defined as the mass (mg) per unit area (cm^2), determined by weighing the membrane samples in their dry state. The results indicate that the mass per unit surface area increases from M1 to M4, indicating that as more PSS was incorporated into the membrane, the density increases, suggesting the effective incorporation of PSS depends on the amounts introduced during synthesis.

Table 3
Physicochemical properties of the membranes

Membrane	Membrane appearance	Density (mg/cm^2)	Contact angle θ (°)
M1	No PSS	5.865	54 ± 0.2
M2	Homogeneous dispersion of PSS	6.077	57 ± 0.2
M3	Homogeneous dispersion of PSS	6.598	69 ± 0.2
M4	Homogeneous dispersion of PSS	7.363	88 ± 0.2

Moreover, the contact angle also increased progressively from M1 to M4. This trend clearly demonstrates an increase in membrane hydrophobicity with higher PSS content. The contact angle ranged from 54° in M1 to 88° in M4, indicating a significant shift towards hydrophobic behavior as the PSS concentration rises. The decline in membrane hydrophilicity observed with the increase in PSS concentration, was probably due to the D2EHPA migration to membranes' surface, structural compaction, and the hydrophilic groups of PSS being covered by intramolecular interactions. These phenomena can be improve by the synthesis method and the redistribution of components upon evaporation.[47] The presence of D2EHPA and the use of the slow solvent evaporation method can significantly influence the hydrophilic or hydrophobic properties of PSS-CTA membranes. These factors play a critical role in determining the structure and final properties of the membranes and could explain the observed decrease in hydrophilicity with increasing PSS concentrations. In fact, D2EHPA contains long hydrophobic alkyl chains, which can dominate the membrane surface properties if they migrate to the surface during membrane formation. This migration can mask the hydrophilic sulfonate groups of PSS, leading to reduced hydrophilicity with increasing PSS concentration. In addition, slow evaporation generally results in a denser and smoother membrane surface, which can limit the accessibility of hydrophilic sites. This dense structure can lead to reduced water interactions.[48]

SEM characterization

The analysis of the different membranes was carried out using scanning electron microscopy (SEM). The SEM images presented in Figure 1 offer a detailed view of the surface morphology of the synthesized membranes, with some characteristics and their implications for membrane performance. SEM images reveal a dense and non-porous surface. Accordingly, the membranes follow a progressive trend in PSS loading, in the order: M1 < M2 < M3 < M4, reflecting the increasing concentrations used during synthesis.

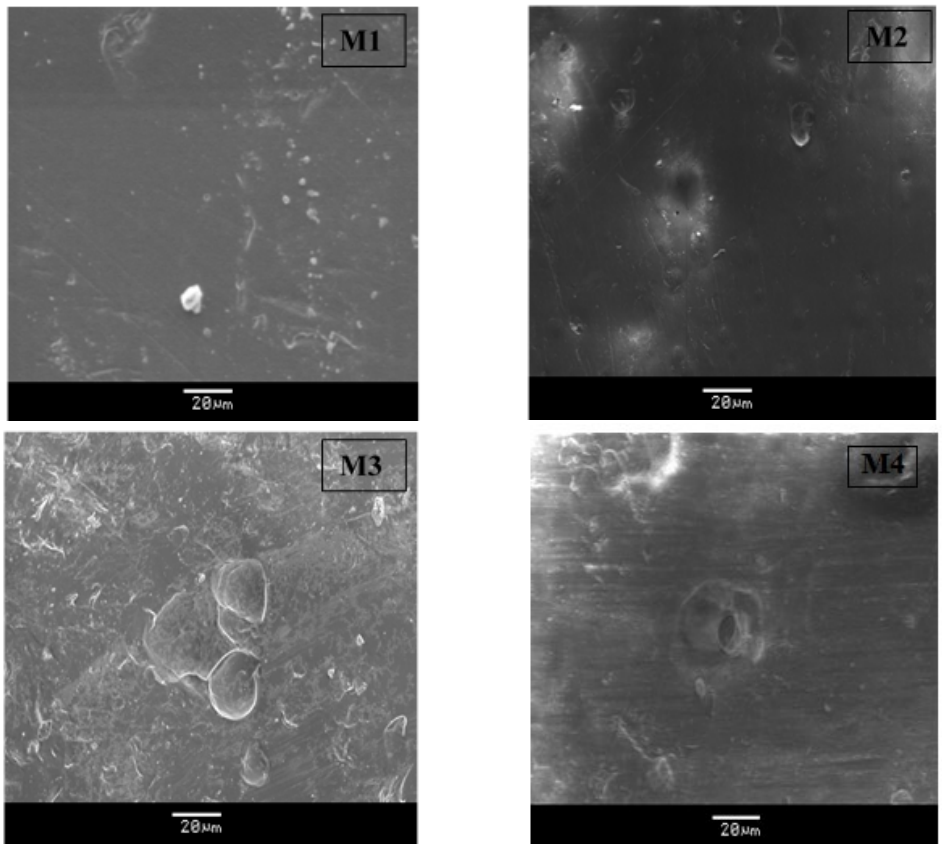

Figure 1: SEM micrographs of membrane surfaces

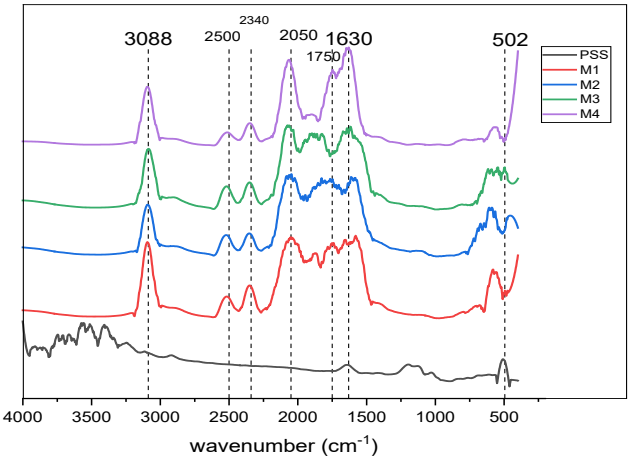

Figure 2: FTIR spectra of membranes and PSS

Table 4
Peak values and their corresponding radicals

Component	Group	Absorption band
PSS	S-C	502 cm^{-1}
CTA	C=O	1750 cm^{-1}
	C-H	3080 cm^{-1}
D2EHPA	O=P-OH	1630 cm^{-1}

This formation can be explained by the slow evaporation process that led to a uniform dense layer on the surface, where the components (CTA and D2EHPA) organized into a compact matrix. Indeed, a slow solidification phase limits the formation of pores during evaporation. Moreover, a strong interaction between CTA and D2EHPA can reduce the mobility of polymer chains and prevent the formation of porous structures. The PSS incorporated in the matrix can act as a morphology modifier by pushing the D2EHPA from the inside to the surface of the membrane. The PSS can be uniformly dispersed, contributing to an increase in membrane density.[49]

FTIR characterization

Cellulose triacetate typically exhibits a strong absorption band around 1730-1750 cm^{-1} due to the ester carbonyl group (C=O stretching). Changes in the position of this band can be attributed to interactions with D2EHPA or PSS. D2EHPA exhibits characteristic bands near 1250-1260 cm^{-1} (P=O stretching). Modifications or absence of these peaks may suggest an interaction with the polymers. PSS typically exhibits absorption bands around 1120-1170 cm^{-1} (S=O stretching) visible in the spectrum of PSS alone. A modification is observed in the spectra of the synthetized membranes, the absence of the characteristic band around 1120 to 1170 cm^{-1} can be attributed to interactions between PSS and CTA or D2EHPA.

The results indicate the successful incorporation of all components into the membranes, with the expected functional groups consistently identified across the samples.

Membranes' application

Transport of Na^+, Ca^{2+} and K^+ ions through membranes

Figures 3–5 show the variation of Na^+, Ca^{2+} and K^+ ions concentrations transferred through membranes to the receiving compartment *versus* time. It may be remarked that the concentration curves of ions transferred through the membranes exhibit a similar trend, regardless of the membrane type. An initial rapid increase is observed during the first 8 hours of dialysis, followed by a gradual slowdown in ion transfer up to 24 hours.

It is also observed that the amount of PSS incorporated into the membrane directly affects its transfer properties. The results indicate that ion transfer increases as the PSS content increases, following the order: M3 > M4 > M2 > M1.

These observations can be explained by the fact that, at the beginning of the dialysis process, an important concentration gradient exists between the compartment containing the initial solution and the receiving compartment, filled with a low-ionic-concentration solution. This strong gradient promotes the rapid diffusion of ions across the semipermeable membrane. Ions with lower charge and smaller hydrated radius, such as K^+, diffuse more quickly than larger, highly hydrated ions, such as Ca^{2+} and Na^+.[50] As ions migrate into the receiving compartment, the concentration gradient between the two compartments decreases, leading to a reduction in diffusion flux. Over time, the system approaches equilibrium as electrostatic and osmotic forces gradually influence the process, further slowing ion transport.

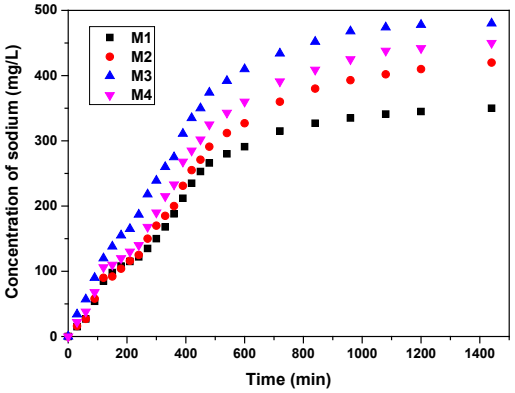

Figure 3: Variation of Na^+ concentration in the strip compartment *versus* time

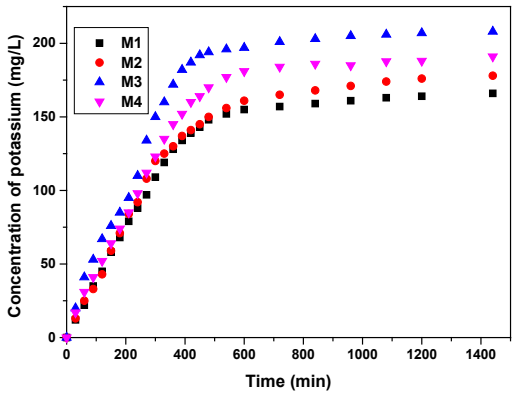

Figure 4: Variation of K^+ concentration in the strip compartment *versus* time

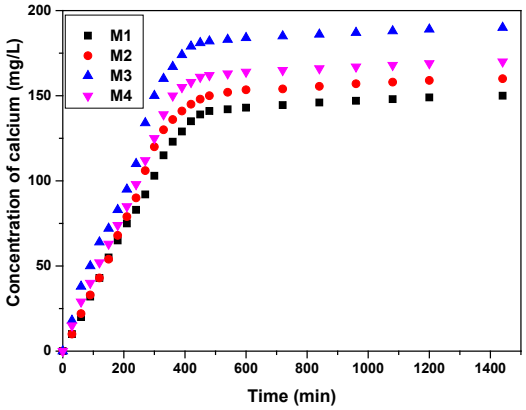

Figure 5: Variation of Ca^{2+} concentration in the strip compartment *versus* time

Membranes can also exhibit saturation phenomena, where the availability of transport sites limits the progression of ionic transfer. In fact, the membranes' structure impacts ion selectivity and diffusion.[51] Membranes–ions interactions, such as adsorption or ion exchange, can slow down the transfer in the long term.

The use of D2EHPA facilitates the capture and transport of calcium at the beginning of the process. Once the complexation sites become saturated, the transfer rate decreases and eventually stabilizes, leading to a plateau in the ionic flux over time.

PSS is a polyanion that imparts a negative charge to membranes. This promotes the passage of cations (K^+, Ca^{2+}, Na^+) due to electrostatic attraction, thereby enhancing the diffusion of positively charged ions. However, an excessive concentration of PSS can lead to membrane densification, which gradually hinders ion diffusion. This phenomenon explains the observed decrease in ion transfer concentration through the M4 membrane over time.

Considering its higher performance, membrane M3, containing 0.02 g of PSS polymer, was further tested for treating seawater solutions previously filtered using sand. The results obtained during

these tests were presented in Figure 6. It may be noticed that the shape of the ion transfer curves (K^+, Ca^{2+}, Na^+) through the M3 membrane is the same as in the case of synthetic solutions, which indicates that the membrane is mostly stable, despite the complexity of the solution treated. Again, an initial rapid increase is observed during the first 8 hours of dialysis, followed by a gradual slowdown in ion transfer up to 24 hours.

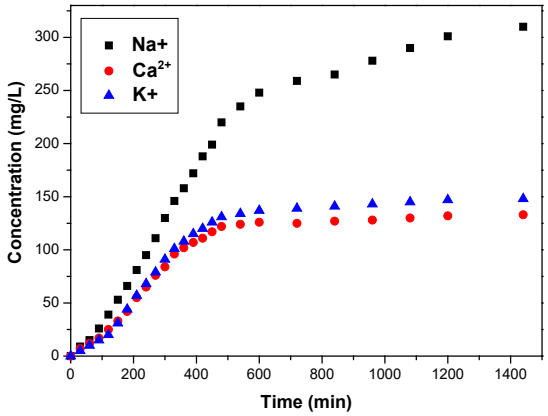

Figure 6: Variation of ion concentrations in the strip compartment *versus* time using seawater solution and M3 membrane

Ion flux and permeability coefficient

The ion transport flux was determined by the following equation:

$$J_M = \frac{\Delta m}{S\,\Delta t}\ (\text{mg. cm}^{-2}\ \text{s}^{-1}) \qquad (1)$$

where Δm represents the variation of the quantities of the species in the receiving compartment during time variation Δt, and S is the effective membrane surface area (S = 49 cm²). The relation between the flux in the membrane (J) and the permeability coefficient (P) was determined by:

$$P = \frac{J}{C}\ (\text{cm.s}^{-1}) \qquad (2)$$

where C is total concentration of the species in the feed solution at each time point.

The determination of the flux and permeability coefficient of K^+, Ca^{2+}, Na^+ ions through the membranes confirmed the results already obtained. The M3 membrane containing (0.02 mg of PSS) gives the best results in terms of ion flux and permeability coefficient values.

Table 5
Average flux after 8 hours of dialysis

J_M (mg.cm^{-2} s^{-1})	J_{M1}	J_{M2}	J_{M3}	J_{M4}	J_{M3sw}
Na^+	1.884 10^{-4}	2.062 10^{-4}	2.650 10^{-4}	2.303 10^{-4}	1.550 10^{-4}
K^+	0.999 10^{-4}	1.062 10^{-4}	1.289 10^{-4}	1.147 10^{-4}	0.928 10^{-4}
Ca^{2+}	1.048 10^{-4}	1.077 10^{-4}	1.374 10^{-4}	1.204 10^{-4}	0.864 10^{-4}

Table 6
Permeability coefficients of the membranes

P_{M1} (cm.s^{-1})	P_{M1}	P_{M2}	P_{M3}	P_{M4}	P_{M3sw}
Na^+	1.884 10^{-8}	2.062 10^{-8}	2.650 10^{-8}	2.303 10^{-8}	1.437 10^{-8}
K^+	2.561 10^{-11}	2.723 10^{-11}	3.305 10^{-11}	2.941 10^{-11}	2.361 10^{-11}
Ca^{2+}	2.556 10^{-11}	2.626 10^{-11}	3.351 10^{-11}	2.936 10^{-11}	2.097 10^{-11}

Ion transfer efficiency analysis

The bar charts in Figures 7 and 8 illustrate the ion transfer efficiencies for K^+, Na^+ and Ca^{2+} ions contained in synthetic solution and seawater solution through different synthesized membranes after 6 hours of dialysis process. The results show that M3 membrane has the highest efficiency for all ion transfers, indicating its superior performance in facilitating ion transport, compared to the other membranes, with approximately 49.74%, 44.39%, and 3.74% for K^+, $Ca^{2+}$and Na^+ ions, respectively. The transfer follows the order

M3 >M4> M2 > M1. This can be attributed to its optimal structural properties that enhanced ion mobility. The results further indicate that the introduction of an increased quantity of PSS into the membrane (M4) significantly influences transfer efficiencies. Specifically, a decrease in transfer efficiency is observed. This phenomenon can be attributed to alterations in the membrane's structure and properties, where the PSS polymer potentially occupies and obstructs some of the pores within the membrane matrix.[52,53] This obstruction likely reduces the available pathways for ion transport, thereby decreasing the overall efficiency of the membrane. The change in the membrane's morphology, due to the higher PSS content, suggests that the distribution and concentration of the polymer within the membrane play a crucial role in determining its transport characteristics.

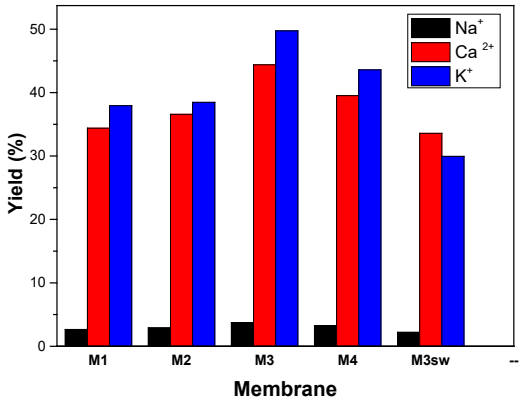

Figure 7: Ion transfer efficiencies after 6 hours of dialysis process

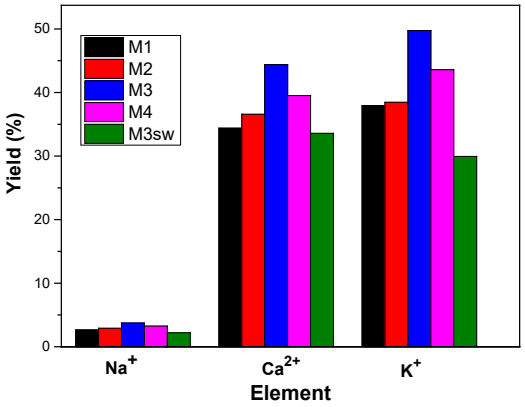

Figure 8: Ion transfer efficiencies after 6 hours of dialysis process

Potassium ions generally exhibit the highest transfer efficiencies across all membranes, followed by sodium and calcium ions respectively, with 33.58%, 29.95%, and 2.20% for K^+, Ca^{2+} and Na^+ ions respectively. This trend suggests that the synthetized membranes have varying affinities and transport mechanism for different ions. The higher efficiency for K^+ ions could be due to their higher mobility compared to Na^+ and Ca^{2+} ions. The observed transfer of potassium ions to the receiving compartment more effectively than calcium and sodium ions during dialysis using membranes composed of PSS, CTA, and DEHPA can be attributed to membranes affinity and the ion radius hydration. Potassium ions (K^+), being monovalent and possessing a lower charge density compared to divalent calcium ions (Ca^{2+}), might interact more favorably with the membrane materials. These interactions could reduce binding strength and increase mobility across the membrane. Also, the hydration radius of potassium ions is smaller compared to sodium and calcium ions. This smaller effective size allows potassium to diffuse more easily through membrane pores or interact efficiently with the functional groups in the membrane.

Results also show that the calcium ions (Ca^{2+}) were transferred more than sodium ions (Na^+). This phenomenon can be explained by the presence of D2EHPA as carrier in the membrane composition. D2EHPA is an organophosphorus extractant that strongly interacts with divalent ions, such as Ca^{2+}. Its incorporation into membranes improves the selectivity for calcium, which explains why Ca^{2+} is better transferred than Na^+.

The application of the seawater solution for the dialysis process using the M3 membrane exhibits lower transfer efficiencies for all ions, compared to the synthetic solution tests, which can be attributed to the complex composition of seawater that may hinder ion transfer because of the presence of other interfering substances or competitive ion interactions. This suggests the need for pretreatment steps to remove competing ions or organic matter.

Table 7 tabulates the seawater characteristics before and after the treatment by the membrane dialysis process using membrane M3.

These findings indicate that integrating the dialysis process with CTA-PSS-D2EHPA membranes as a pretreatment step before RO can effectively reduce salt concentrations and improve

water quality by the diminution of salinity, conductivity and total dissolved solids (TDS) of seawater.

The incorporation of PSS and D2EHPA into the membrane facilitates the migration of ions and small dissolved molecules through the membrane and enhances ion selectivity,[54-56] promoting the transfer of ions such as K^+ and Ca^{2+} from the seawater compartment to the distilled water. Significant reduction in conductivity, salinity and total dissolved solids in the treated solution was observed. This implies reduction in these characteristics in the seawater after treatment, as PSS enables selective passage of dissolved substances, while retaining larger particles or non-ionic species.

Table 7
Seawater solution caracteristic before and after treatment

	Conductivity ($mS.cm^{-1}$)	pH	Salinity ($g.L^{-1}$)	TDS ($g.L^{-1}$)	Turbidity (NTU)	Dissolved oxygen (mg/L)
Before treatment	51.4	7.34	32.9	33.4	0.51	3.6
After treatment	39.7	7.11	26.64	25.43	0.34	9.3

There was a slight reduction in turbidity after treatment, but this reduction is limited. The PSS-modified dialysis membrane primarily facilitates the transfer of ions and small molecules and is not specifically designed to filter out suspended particles, which contribute to turbidity. PSS, although effective for ion exchange, does not directly aid in the filtration of undissolved particles. This explains why turbidity remains relatively high after treatment. The slight decrease in pH after the treatment was likely due to the acidic sulfonate groups in PSS, which can interact with certain ions or release small quantities of protons (H^+) into the solution.[57] However, this change is moderate and does not indicate any significant imbalance in the acidity of the treated solution.

The substantial increase in dissolved oxygen (DO) can be attributed to improved oxygenation of the seawater after passing through the dialysis membrane. The removal of solutes and ions by the PSS-modified membrane likely reduces the oxygen demand in the water, as less organic matter or contaminants that consume oxygen remain after the treatment. This leads to a significant increase in oxygen levels in the treated solution.

CONCLUSION

The performance of membrane desalination processes largely depends on the effectiveness of the pretreatment steps used. This study explores the integration of a low-energy process aimed at improving pretreatments by reducing the salt concentration of seawater intended for reverse osmosis (RO). New polymer membranes were developed, characterized and tested using the dialysis process.

These membranes were synthesized from cellulose triacetate (CTA), modified by using polystyrene sulfonate (PSS), and plasticized with di-(2-ethylhexyl) phosphoric acid (D2EHPA). SEM characterization has shown that membranes have a dense and amorphous structure, while PSS integration into the membrane matrix can act as a morphology modifier by pushing the D2EHPA from the inside to the surface of membrane. FTIR spectra indicated the successful incorporation of all components into the membranes. Membranes application results demonstrates significant reductions in ion concentrations when using the CTA+PSS+D2EHPA membrane, with 33.58%, 29.95%, and 2.20% for K^+, Ca^{2+} and Na^+ ions, respectively, using seawater solutions. The membrane containing PSS effectively facilitates the transfer of ions, reducing conductivity, salinity, and TDS in the treated solution. PSS also improves oxygenation, leading to higher dissolved oxygen levels, but has little effect on turbidity, which remains relatively high. The pH is slightly influenced by the acidic groups in PSS, but remains within acceptable limits for seawater conditions.

These findings indicate that integrating the dialysis process with CTA-PSS-D2EHPA membranes can effectively reduce Ca^{2+} concentration in saline solution, considered as responsible for membrane scaling phenomena. This method is not only effective, but also energy-efficient and cost-effective. The enhanced performance is attributed to the optimized membrane properties resulting from the inclusion of PSS, which increases ion transfer efficiencies.

REFERENCES

[1] W. L. Filho, E. Totin, J. A. Franke, S. M. Andrew, I.

Abubakar *et al*., *Sci. Total Environ*., **806**, 150420 (2022), https://doi.org/10.1007/s11743-016-1884-x
[2] A. C. Ahmia, M. Idouhar, O. Arous, K. Sini, A. Ferradj *et al*., *J. Surfact. Deterg*., **19**, 1305 (2016), https://doi.org/10.1016/j.jeem.2022.102633
[3] C. He, Z. Liu and J. Wu, *Nat. Commun*., **12**, 4667 (2021), https://doi.org/10.1038/s41467-021-25026-3
[4] M. Ayaz, M. A. Namazi, M. Ammad ud Din, M. I. M. Ershath, A. Mansour *et al*., *Desalination*, **540**, 116022 (2022), https://doi.org/10.1016/j.desal.2022.116022
[5] N. Ghaffour, T. M. Missimer and G. L. Am, *Desalination*, **309**, 197 (2013), http://dx.doi.org/10.1016/j.desal.2012.10.015
[6] V. A. Tzanakakis, N. V. Paranychianakis and A. N. Angelakis, *Water Suppl. Water Scarc*., **12**, 2347 (2020), https://doi.org/10.3390/w12092347
[7] V. Khilchevskyi and V. Karamushka, "Global Water Resources: Distribution and Demand. Clean Water and Sanitation", Springer, Cham, 2021, https://doi.org/10.1007/978-3-319-70061-8101-1
[8] C. Ingrao, R. Strippoli, G. Lagioia and D. Huisingh *Heliyon*, **9**, 18507 (2023), https://doi.org/10.1016/j.heliyon.2023.e18507
[9] A. Liponi, C. Wieland and A. Baccioli, *Energ. Convers. Manage*., **205**, 112337 (2020), https://doi.org/10.1016/j.enconman.2019.112337
[10] S. Aly, H. Manzoor, S. Simson, A. Abotaleb, J. Lawler *et al*., *Desalination*, **519**, 115221 (2021), https://doi.org/10.1016/j.desal.2021.115221
[11] A. J. Toth, *Membranes*, **10**, 265 (2020), https://doi.org/10.3390/membranes10100265
[12] M. A. Hafiz, R. Alfahel, A. Altaee and A. H. Hawari, *Sep. Purif. Tech*., **309**, 123007 (2023), https://doi.org/10.1016/j.seppur.2022.123007
[13] A. Matin, T. Laoui, W. Falath and M. Farooque, *Sci. Total Environ*., **765**, 142721 (2021), https://doi.org/10.1016/j.scitotenv.2020.142721
[14] K. Harby, M. Emad, M. Benghanem, T. Z. Abolibda, K. Almohammadi *et al*., *Desalination*, **581**, 117600 (2024), https://doi.org/10.1016/j.desal.2024.117600
[15] J. Wu, J. He, J. A. Quezada-Renteria, J. Le, K. Au *et al*., *J. Membr. Sci*., **706**, 122893 (2024), https://doi.org/10.1016/j.memsci.2024.122893
[16] Y. J. Lim, K. Goh, M. Kurihara and R. Wang, *J. Membr. Sci*., **629**, 119292 (2021), https://doi.org/10.1016/j.memsci.2021.11929
[17] D. L. Zhao, S. Japip, Y. Zhang, M. Weber, C. Maletzko *et al*., *Water Res*., **173**, 115557 (2020), https://doi.org/10.1016/j.watres.2020.115557
[18] M. M. Tawalbeh, L. Qalyoubi, A. Al-Othman, M. Qasim and M. Shirazi, *Desalination*, **553**, 116460 (2023), https://doi.org/10.1016/j.desal.2023.116460
[19] G. Sert, S. Bunani, E. Yörükoğlu, N. Kabay, Ö. Egemen *et al*., *J. Water Proc. Eng*., **16**, 193 (2017), https://doi.org/10.1016/j.jwpe.2016.11.009
[20] R. H. Hailemariam, Y. C. Woo, M. M. Damtie, B. C. Kim, K. D. Park *et al*., *Adv. Colloid Interface Sci*., **276**, 102100 (2020), https://doi.org/10.1016/j.cis.2019.102100
[21] M. Badruzzaman, N. Voutchkov, L. Weinrich and J. G. Jacangelo, *Desalination*, **449**, 78 (2019), https://doi.org/10.1016/j.desal.2018.10.006
[22] J. Kavitha, M. Rajalakshmi, A. R. Phani and M. Padaki, *J. Water Proc. Eng*., **32**, 100926 (2019), https://doi.org/10.1016/j.jwpe.2019.100926
[23] N. Voutchkov, *Desalination*, **261**, 354 (2010), https://doi.org/10.1016/j.desal.2010.07.002
[24] A. B. Mohammed, A. K. S. Raju, J. Lee, Y. Oh and S. Jeong, *J. Environ. Chem. Eng*., **9**, 106784 (2021), https://doi.org/10.1016/j.jece.2021.106784
[25] N. Chekir, D. Tassalit and N. Sahraoui, *Chem. Pap*., **78**, 9473 (2024), https://doi.org/10.1007/s11696-024-03759-x
[26] S. Brover, Y. Lester, A. Brenner and E. Sahar-Hadar, *Desalination*, **524**, 115478 (2022), https://doi.org/10.1016/j.desal.2021.115478
[27] G. Q. Chen, Y. H. Wu, P. S. Fang, Y. Bai, Z. Chen *et al*., *J. Membr. Sci*., **641**, 119850 2022, https://doi.org/10.1016/j.memsci.2021.119850
[28] M. Verma and V. A. Loganathan, *J. Water Proc. Eng*., **64**, 105706 (2024), https://doi.org/10.1016/j.jwpe.2024.105706
[29] Z. Wu, W. Qiao, Y. Liu, J. Yao, C. Gu *et al*., *J. Membr. Sci*., **647**, 120298 (2022), https://doi.org/10.1016/j.memsci.2022.120298
[30] S. Park, M. Saavedra, X. Liu, T. Li, B. Anger *et al*., *J. Membr. Sci*., **694**, 122399 (2024), https://doi.org/10.1016/j.memsci.2023.122399
[31] O. Arous, A. Gherrou and H. Kerdjoudj, *Sep. Sci. Technol*., **39**, 1681 (2005), https://doi:10.1081/SS-120030792
[32] F. Benhacine, N. Abdellaoui, O. Arous and A. S. Hadj-Hamou, *Environ. Technol*., **41**, 2049 (2020), https://doi:10.1080/09593330.2018.1555283
[33] F. Smail, O. Arous, M. Amara and H. Kerdjoudj, *Comptes Rendus Chimie*, **16**, 605 (2013), https://doi.org/10.1016/j.crci.2013.04.003
[34] N. Abdellaoui, F. M. Laoui, H. Cerbah and O. Arous, *J. Appl. Polym. Sci*., **135**, 46592 (2018), https://doi.org/10.1002/app.46592
[35] N. Abdellaoui, Z. Himeur and O. Arous, *Macromol. Symp*., **386**, 1800240 (2019), https://doi.org/10.1002/masy.201800240
[36] H. Briki, N. Abdellaoui, F. Metref, D. E. Akretche and O. Arous, *J. Biotech. Biores*., **2**, 1 (2020), https://doi.10.31031/JBB.2020.02.000539
[37] H. Briki, N. Abdellaoui, O. Arous, F. Metref and D. E. Akretche, *Cellulose Chem. Technol*., **56**, 1109 (2022), https://doi.org/10.35812/CelluloseChemTechnol.2022.56.99
[38] G. Lainioti, G. Bounos, G. A. Voyiatzis and J. K. Kallitsis, *Polymers*, **8**, 190 (2016), https://doi.10.3390/polym8050190

[39] H. Li, S. Zhang, B. Sengupta, F. Wang, S. Li *et al*., *J. Membr. Sci*., **657**, 120617 (2022), https://doi.org/10.1016/j.memsci.2022.120617
[40] X. Q. Cheng, S. Li, H. Bao, X. Yang, Z. Li *et al*., *Adv. Compos. Hyb. Mat*., **562**, 573 (2021), https://doi.org/10.1007/s42114-021-00253-w
[41] A. Krishna, H. J. Zwijnenberg, S. Lindhoud and W. M. de Vos, *J. Membr. Sci*., **652**, 120463 (2022), https://doi.org/10.1016/j.memsci.2022.120463
[42] S. U. Baowei, T. Wang, Z. Wang, X. Gao and C. Gao, *J. Membr. Sci*., **423**, 324 (2012), https://doi.org/10.1016/j.memsci.2012.08.041
[43] C. Dong, R. He, S. Xu, H. He, H. Chen *et al*., *Desalination*, **534**, 115793 (2022), https://doi.org/10.1016/j.desal.2022.115793
[44] M. Yu, T. X. Ren, X.G. Jin, X. Tang, M. M. Tang *et al*., *Desalination*, **580**, 117561 (2024), https://doi.org/10.1016/j.desal.2024.117561
[45] B. Zhou, J. Luo, R. Li, R. He and T. He, *Desalination*, **581**, 117602 (2024), https://doi.org/10.1016/j.desal.2024.117602
[46] M. Sugiura, M. Kikkawa and S. Urita, *J. Membr. Sci*., **42**, 47 (1989), https://doi.org/10.1016/S0376-7388(00)82364-9
[47] Y. Sedkaoui, N. Abdellaoui, O. Arous, H. Lounici, N. Nasrallah *et al*., *J. Polym. Eng*., **41**, 127 (2021), https://doi.org/10.1515/polyeng-2020-0165
[48] S. Bensadi, N. Drai, O. Arous, Y. Berbar, Z. E. Hammache *et al*., *J. Memb. Sci. Res*., **8**, 1 (2022), https://doi.org/10.22079/JMSR.2021.531653.1470
[49] J. Wang, W. Zhang and W. Li, *Korean J. Chem. Eng*., **32**, 1369 (2015), https://doi.org/10.1007/s11814-014-0328-4
[50] Z. Qian, H. Miedema, L. C. P. M. de Smet and E. J. R. Sudhölter, *Desalination*, **521**, 115398 (2022), https://doi.org/10.1016/j.desal.2021.115398
[51] P. Grzybek, G. Dudek and B. Van der Bruggen, *Chem. Eng. J*., **495**, 153500 (2024), https://doi.org/10.1016/j.cej.2024.153500
[52] J. Wang, X. Lv and L. Huang, *Korean J. Chem. Eng*., **40**, 175 (2023), https://doi.org/10.1007/s11814-022-1236-7
[53] M. Yu, T. X. Ren, X. G. Jin, X. Tang, M. M. Tang *et al*., *Desalination*, **580**, 117561 (2024), https://doi.org/10.1016/j.desal.2024.117561
[54] X. Tong, S. Liu, Y. Zhao, L. Huang, J. Crittenden *et al*., *Environ. Sci. Technol*., **56**, 8964 (2022), https://doi.org/10.1021/acs.est.2c01765
[55] Y. Zhao, M. Wu, Y. Guo, N. Mamrol, X. Yang *et al*., *J. Membr. Sci*., **634**, 119407 (2021), https://doi.org/10.1016/j.memsci.2021.119407
[56] F. A. Khanghah, J. Karimi-Sabet and C. Ghotbi, *Chem. Eng. Res. Design*., **191**, 353 (2023), https://doi.org/10.1016/j.cherd.2023.01.029
[57] A. F. Elerian, A. A. Mohamed and E. M. Elnaggar, *Polym. Bull*., **81**, 17177 (2024), https://doi.org/10.1007/s00289-024-05487-4